Elucidation of Charge Contribution in Iridium-Chelated Hydrogen-Bonding Systems

Barbora Balónová and Barry A. Blight*

Department of Chemistry, University of New Brunswick, Fredericton, New Brunswick, Canada, E3B 5A3.

Barry A Blight
b.blight@unb.ca

Abstract

We present two iridium complexes **1H$^+$** and **2H$^+$** that contain cationic ligands to extend the knowledge of charge-assisted hydrogen bonding (CAHB), which counts among the strongest non-covalent bonding interactions. Upon protonation, both complexes were converted into new hydrogen-bonding arrays with various selectivity for respective H-bonding partners. This study compares the association strengths of four hydrogen-bonding co-systems, emphasizing the roles of CAHB in supramolecular systems. We determined that the cationic charge in these systems contributed up to 2.7 kJ mol^{-1} in the H-bonding complexation processes.

1   Introduction

Hydrogen-bonding is a type of interaction that plays a crucial role in most branches of science (Marechal, 2007). Not surprisingly, this interaction is often used in biochemical processes (Moran et al., 2012), materials science (Chowdary and Gillespie, 2018), and many applicative areas of supramolecular chemistry (Kuhn et al., 2010; Persch et al., 2015). The electrostatic interaction occurs between the partial positively charged hydrogen atom X-H (donor) and a partial negatively charged hydrogen acceptor atom Y, where X and Y are electronegative atoms (such as N, O, or S). In addition to hydrogen bonds (H-bonds), supramolecular systems can be reinforced by the cooperative interactions between binding partners in the assembly (Prins et al., 2001). An important example of this statement is charge-assisted H-bonding (CAHB), which can be described as an interaction of the X-H$^+$···Y$^-$ type, where the X-H donor belongs to the cation, and the Y acceptor belongs to the anion. Here, the charge assisted bonds X-H$^+$···Y$^-$, also known as a salt bridge, combine the inherent strength

28   and directionality of the hydrogen bond with favorable localization of the ionic charges while being
29   easily obtained via an acid-base reaction (Braga et al., 2000). Previously reported strategies for the
30   preparation of CAHB systems often involve strategies incorporating nitrogen-based compounds
31   (amines, amides, amidines), which can accept a proton from a carboxylic acid, for example, leading to
32   the formation of $N-H^+\cdots O^-$ interactions (Papoutsakis et al., 1999; Félix et al., 2000; Schmuck and
33   Wienand, 2003) with free energies ranging from 4.0 - 5.2 kJ mol^{-1} (Horovitz et al., 1990).

34   Leigh and coworkers presented quadruple hydrogen-bonding complexes, including protonated salts
35   with four $N-H\cdots N$ interactions that include an ion-dipole $N-H^+\cdots N$ array (Leigh et al., 2013). These
36   interactions can be switched on/off by the controlled addition of acid and base (Blight et al., 2011).
37   Such configurations may be useful for designing responsive materials, such as nanofibers, gels, and
38   supramolecular polymers. CAHBs tend to possess stronger interactions than a simple hydrogen bond
39   due to the additional electrostatic interaction involved, resulting from one or more of the components
40   bearing a charge (Papmeyer et al., 2016; Pop et al., 2016). Experimental deconvolution of sole-charge
41   contribution in CAHB systems has yet to be quantified in assemblies where multiple hydrogen bonding
42   arrays are employed. Several reports have shown that CAHB systems have found application in crystal
43   engineering (Liu et al., 2019), synthesis of pharmaceutical salts/co-crystals (Wang et al., 2014), and in
44   organometallic systems (Braga et al., 2004), making the elucidation of this energetic contribution
45   critical in predicting materials properties.

46   In this study, we explore the effect of CAHB through the protonation of guanidine and thiourea-based
47   ligands. According to the study conducted by Taylor and Kennard, N-H donors with a formal positive
48   charge tend to form shorter bonds than uncharged N-H groups (Taylor and Kennard, 1984), which
49   indicates a stronger association strength. Guanidinium derivatives represent a versatile functional
50   group with unique properties (Blondeau et al., 2007; Han et al., 2008; Gale et al., 2013), and together
51   with thiourea derivatives (Lee et al., 2002), have been widely investigated as part of the supramolecular
52   systems. As such, we present here a comprehensive study of non-covalent self-assembly of the ionic
53   iridium (III) complexes **1H$^+$** and **2H$^+$** (illustrated in Figure 1) with two different guest molecules **3**
54   (Balónová et al., 2018) and **4** (Blight et al., 2009). These cationic complexes were found to exhibit
55   stronger association constants than with the neutral species **1** (Balónová et al., 2018) and **2** (Balónová
56   et al., 2020) when combined with complementary binding partners **3** and **4**. Chelation of the iridium
57   (III) center by the guanidine and thiourea ligands eliminates any destructive rotational energy allowing
58   us to accurately determine the contribution of the cationic charge to the association strength *via*
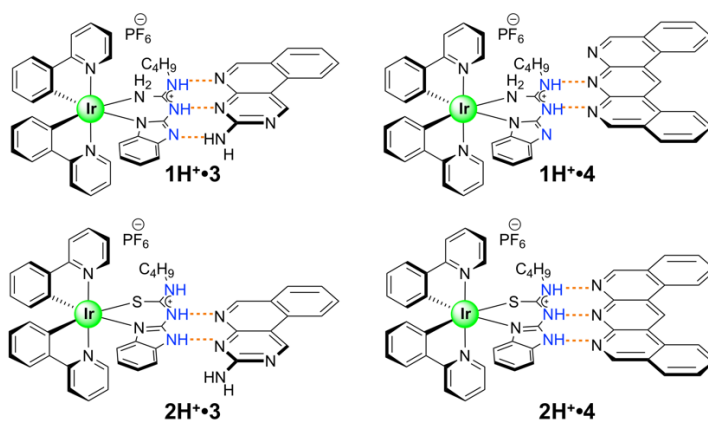59   experimentation.

Figure 1. Four complimentary charge-assisted H-bonding systems featured in this study.

2   Results and Discussion

We have previously reported the synthesis and characterization data of thiourea and guanidine-based ligands used for the synthesis of iridium complexes **1H⁺** and **2H⁺** (Balónová et al., 2018; Balónová et al., 2020). Synthetic details for cationic complexes **1H⁺** and **2H⁺** are presented in the supplementary material for this article (SM, see section S1). Iridium μ-chloro-bridged dimer [Ir(ppy)$_2$Cl]$_2$ (ppyH = phenylpyridine) dimer was prepared by the procedure reported by Nonoyama (Nonoyama, 1974). Complex **1H⁺** was synthesized using 1-(1H-benzo[d]imidazole-2-yl)-3-butylguanidine as a ligand followed by the ligand exchange using potassium hexafluorophosphate (KPF$_6^-$) as the source of PF$_6^-$ counterion. Iridium complex **2H⁺** was synthesized by refluxing 1-(1H-benzo[d]imidazole-2-yl)-3-butylthiourea ligand with the iridium μ-chloro-bridged dimer [Ir(ppy)$_2$Cl]$_2$ in toluene, and similarly followed by the ion exchange with KPF$_6^-$ counterion for the cationic complex **2H⁺**. Complexes **1H⁺** and **2H⁺** were paired with binding partners **3** and **4** (Figure 1), and association constants were determined. UV-vis absorption spectroscopy titration methods were used to measure the association constants for complexes **1H⁺•3/4** and **2H⁺•3/4**, and all data were analyzed with the program BindFit (Thordarson, 2011; SM, see section S5). The titrations were carried out in HPLC grade CHCl$_3$ with 1% of DMSO to support the solubility of binding partners **3** and **4**. The self-association (K_d) of compounds **3** and **4** was determined to be $K_d < 50$ M^{-1} and considered negligible for this study.

81 **Table 1.** Experimentally determined association constants for $1H^+$ and $2H^+$ with two different guest

82 molecules, **3** and **4**, and their neutral parent complexes.

Co-system	Association Constant[a] (K_a)	-ΔG (kJ mol^{-1})	Sartorius (kJ mol^{-1})
1•3	$K_{11} = 8.9 \times 10^5$ M^{-1}	33.9	23.7
	$K_{12} = 4.7 \times 10^3$ M^{-1}	20.9	-
1•4	$K_{11} = 9.9 \times 10^4$ M^{-1}	28.5	21.6
	$K_{12} = 4.2 \times 10^3$ M^{-1}	20.7	-
1H$^+$•3	$K_{11} = 1.1 \times 10^6$ M^{-1}	34.4	23.7
	$K_{12} = 2.1 \times 10^3$ M^{-1}	18.9	-
1H$^+$•4	$K_a = 1.5 \times 10^3$ M^{-1}	18.1	21.6
2•3[b]	$K_a = 2.1 \times 10^3$ M^{-1}	19.0	23.7
2•4[b]	$K_a = 1.6 \times 10^3$ M^{-1}	18.3	21.6
2H$^+$•3	$K_a = 4.8 \times 10^3$ M^{-1}	21.0	21.6
2H$^+$•4	$K_{11} = 2.0 \times 10^4$ M^{-1}	24.5	35.3
	$K_{12} = 8.6 \times 10^3$ M^{-1}	22.4	-

83 [a]Measured by UV-vis absorption spectroscopy in CHCl$_3$ / DMSO (99:1 v/v), 298 K.
84 [b] Data from previously reported work (Balónová et al., 2020).

85

86   Cationic guanidine-based complex $1H^+$ was paired with binding partners **3** and **4,** and association

87 constants were determined through UV-vis absorption titration studies, with results summarized in

88 Table 1. Due to the increased acidity of NH protons in the guanidinium moiety in complex $1H^+$, higher

89 association constants were expected for systems $1H^+$•**3/4** in comparison to the association constants

90 for thiourea based systems $2H^+$•**3/4**. Gibbs free energies for all co-systems, together with the predicted

91 energy values from the empirical model, are also presented in Table 1. Titration study for co-system

92 $1H^+$•**3** (Figure 2; SM, see section S5) revealed slightly increased association constants $K_{11} = 1.1 \times 10^6$

93 M^{-1} and $K_{12} = 2.1 \times 10^3$ M^{-1} (UV-vis, CHCl$_3$ / DMSO, (99:1 v/v)) in comparison to neutral system **1•3**

94 (Table 1). To our surprise, experimental results obtained from UV-vis absorption titration studies with

95 binding partner **4** did not align with our hypothesis. Admittedly, the association strength for protonated

96 co-system $1H^+$•**4** (DDD$^+$-AAA array) – where protonation of the benzimidazole would lead to a DDD$^+$

97 system, a perfect complement to **4** – did not increase compared to neutral co-system **1•4** (DDA-AAA

98   array). As reported by Wisner and coworkers, the association rate can be decreased or increased by

99   changing the structure of the interacting site to the other isomeric form (Linares Mendez et al., 2019).

100   We posit that prototropy of the guanidinium ligand, made possible by the multiple basic sites that

101   guanidine offers, gives rise to a protonated state that does not give rise to the desired DDD[+]

102   arrangement, but an ADD[+] array, as evidenced by the lower-than-expected association constant for

103   **1H[+]•4**, with a modest increase of binding strength observed for **1H[+]•3**.
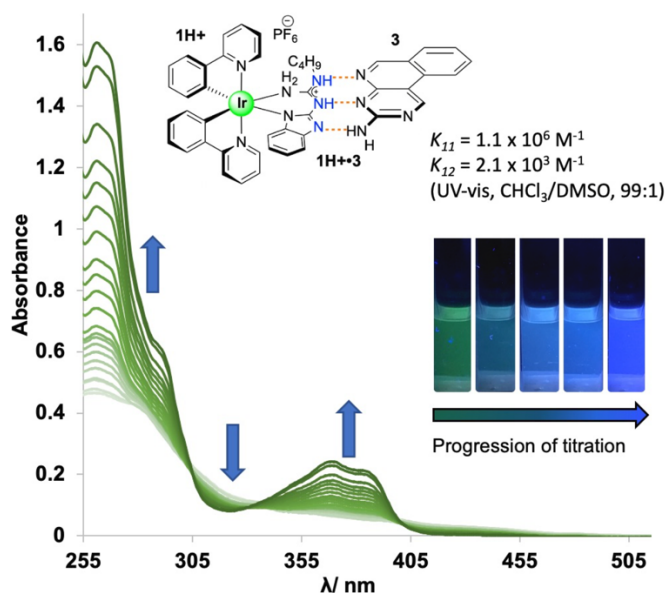

104

105   **Figure 2.** UV-vis absorbance spectra from a titration experiment (298 K) for co-system **1H[+]•3** in CHCl$_3$

106   / DMSO (99:1 v/v).

107

108   Compound **2H[+]** was separately paired with guests **3** and **4**, and their interactions were examined

109   through UV-vis spectroscopic analysis (SM, see section S5) to quantify their respective association

110   constants and compared with neutral systems **2•3** and **2•4** (Table 1). The co-system **2H[+]•3** can be

111   described as a double bonding DD[+]-AA motif with three attractive and one repulsive secondary

112   interaction within the structure. The strength of this association was assessed via UV-vis absorption

113   titration of **2H[+]** with **3** in CHCl$_3$/ DMSO (99:1 v/v), revealing an association constant $K_a = 4.8 \times 10^3$

114   M^{-1} ± 0.4% and the binding energy of -21.6 kJ mol^{-1}, which is almost identical to the value obtained

115   from the Sartorius empirical model that assigns weighted interaction values as the number of

116   interactions increase (Sartorius and Schneider, 1996). This value is almost doubled compared to the

117   neutral co-system **2•3**, which can be explained by the increased number of attractive secondary

118   interactions and electrostatic-charge assistance contributing to the stability and binding energy of the

5

119   **2H⁺•3** system (Table 1). The association constant for co-system **2H⁺•4** was also investigated, and

120   according to the strong influence of secondary interactions, the complementary DDD⁺-AAA system

121   was predicted to be among the most stable arrays presented in this study. As has been previously

122   investigated (and noted above), the binding strength is maximized if all the donor atoms are located on

123   one component and all acceptor atoms are on the binding partner (Jorgensen and Pranata, 1990; Pranata

124   et al., 1991). The planar compound **4** has been previously reported to improve stability and give rise to

125   high association constants in triple DDD-AAA systems (Blight et al., 2009). The neutral complex **2**

126   formed a double H-bonding DD-AA array with **4** (K_a = 1.6 x 10^3 M^{-1} ± 0.1%; Figure 2), and through

127   simple protonation, the multiplicity was increased to triple H-bonding DDD⁺-AAA system **2H⁺•4**.

128   Multiple examples of DDD-AAA complexes have been reported to date (only two DDD⁺), but none of

129   them considered thiourea ligands as binding partners in the assemblies (Balónová et al., 2020;

130   Djurdjevic et al., 2007). Addition of **4** to **2H⁺** in CHCl₃ / DMSO (99:1 v/v) was monitored by UV-vis

131   absorption titration analysis and association constants K_{11} = 2.0 x 10^4 M^{-1} ± 0.1%, K_{12} = 8.6 x 10^3 M^{-1}

132   ± 0.2% for co-system **2H⁺•4** were determined (confirmed by ¹H NMR; Figure 3; SM, see sections S4

133   and S5). Compared to the neutral co-system **2•4**, protonation of complex **2** resulted in ~ 12-fold

134   increase in the association constant when combined with compound **4** in CHCl₃ / DMSO (99:1 v/v).
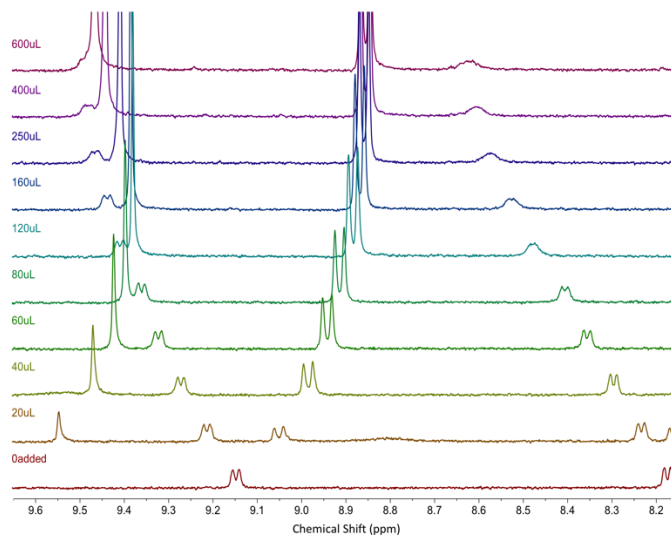

135

Figure 3. Stacked ¹H NMR (400 MHz, 298 K) spectra from titration experiment for co-system **2H⁺•4**

137   in CDCl₃ / DMSO-d_6 (99:1 v/v). **4** (c = 1x10⁻³ M) was titrated into a solution of **2H⁺** (c = 1x10⁻⁴ M) in

138   CDCl₃ / DMSO-d_6 (99:1 v/v).

139   Based on these results, we were able to use an empirical approach to calculate the contribution of

140   charge to the association strength for two of our systems. Protonation of **1H** gives rise to the **1H⁺**,

6

where complex prototropy inhibits identification of the extra proton location. Given that there is a large increase in K_a for $\textbf{1H}^+\textbf{•3}$ and not for $\textbf{1H}^+\textbf{•4}$, which would represent a DDD$^+$-AAA array, we propose that $\textbf{1H}^+\textbf{•3}$ exists as an ADD$^+$ array (vs. DDD$^+$) complemented by $\textbf{3}$ (DAA; Figure 4a), which allows us to directly compare its K_a with that of $\textbf{1H•3}$ (ADD-DAA) given that they have the same number of primary H-bonds and secondary electrostatic interactions. Comparing the neutral guanidine-based co-system $\textbf{1•3}$ ($\Delta G_{1:1}$ = -33.9 kJ mol^{-1}) with the cationic $\textbf{1H}^+\textbf{•3}$ ($\Delta G_{1:1}$ -34.4 kJ mol^{-1}), we calculated the overall charge contribution to the association, as the difference in Gibbs free energy, to be -0.5 kJ mol^{-1}(-0.12 kcal mol^{-1}). As presented in Figure 4b, thiourea-based systems $\textbf{2•4}$ and $\textbf{2H}^+\textbf{•3}$ empirically have the same number of primary hydrogen bonds and attractive/repulsive secondary interactions within the structures, assuming that the different secondary electrostatic interactions contribute equally. Based on this structural arrangement, the charge contribution was calculated. From the comparison of neutral thiourea-based co-system $\textbf{2•4}$ (ΔG = -18.3 kJ mol^{-1}) with the cationic $\textbf{2H}^+\textbf{•3}$ (ΔG = -21.0 kJ mol^{-1}) we calculated the charge contribution in this instance to be -2.7 kJ mol^{-1}(-0.65 kcal mol^{-1}). To the best of our knowledge, discrete charge contribution to association strength in H-bonding arrays has never been determined before. If comparing the Gibbs free energy of charge contribution to salt bridges as determined by Horowitz and coworkers (4.0 - 5.2 kJ mol^{-1}; Horovitz et al., 1990) the charge contributions elucidated in this study are in agreement, given that the present study includes only one of the charged partners.
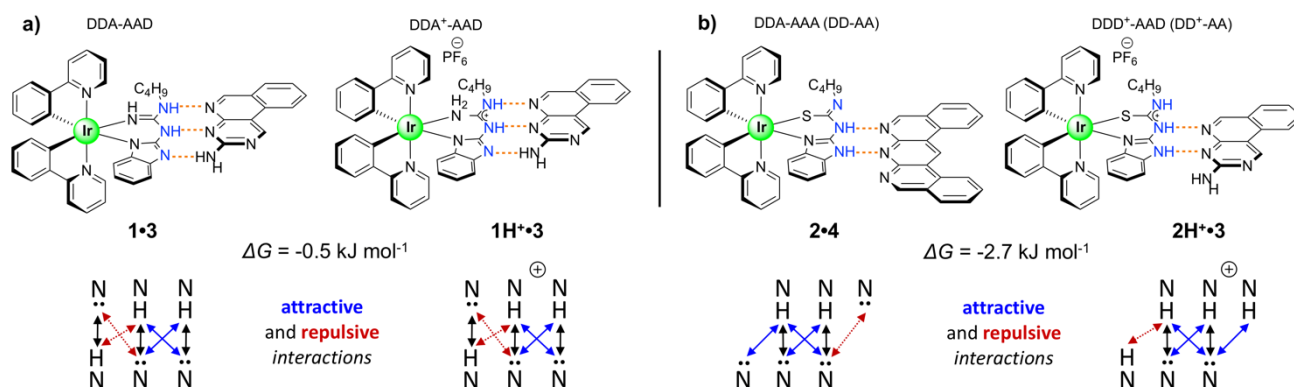

Figure 4. Structural comparison of co-systems a) $\textbf{1•3}$ and $\textbf{1H}^+\textbf{•3}$ and b) $\textbf{2•4}$ and $\textbf{2H}^+\textbf{•3}$ toward experimentally elucidating the charge contribution to these association events.

In summary, we prepared two new cationic iridium (III) complexes $\textbf{1H}^+$ and $\textbf{2H}^+$. Both complexes $\textbf{1H}^+$ and $\textbf{2H}^+$ represent rare examples of charged complexes where the ancillary ligand carries the formal charge (ligand non-innocence). This work further examined the self-assembly of complexes $\textbf{1H}^+$ and

166 **2H$^+$** with guest molecules **3** and **4**, respectively, to determine the charge contribution to the association

167 strength. Guanidine based complex **1H$^+$** with component **3** in DDA-AAD alignment represents the

168 strongest H-bonding system (K_{11} = 1.1 x 10^6 M^{-1} and K_{12} = 2.1 x 10^3 M^{-1}, UV-vis, CHCl$_3$ / DMSO,

169 (99:1 v/v)) in this study due to increased acidity of NH protons in the cationic **1H$^+$** system. In addition,

170 simple protonation of thiourea-based complex **2** results in a ~12-fold increase in the association

171 strength of co-system **2H$^+$•4** in comparison to its neutral version **2•4**. Furthermore, from UV-vis

172 absorption titration studies, we were able to determine the contribution of the charge to the association

173 strength by comparing neutral systems **1•3** and **2•4** with their respective compliments **1H$^+$•3** and **2H$^+$•3**

174 (0.5 kJ mol^{-1} (-0.12 kcal mol^{-1}) and -2.7 kJ mol^{-1} (-0.65 kcal mol^{-1}), respectively). Elucidating the

175 energetics of CAHB interactions will contribute to developing empirical models that allow for more

176 accurate prediction of system dynamics. Based on these results, incorporating CAHB interactions into

177 H-bonding arrays can increase association strengths, leading to higher-order materials and a significant

178 role in more competitive and complex systems.

179

Conflict of Interest

181 The authors declare that the research was conducted in the absence of any commercial or financial

182 relationships that could be construed as a potential conflict of interest.

Author Contributions

184 The manuscript was written through the contributions of all authors. Both authors have given

185 approval to the final version of the manuscript.

ORCID and Twitter:

191 Barry A Blight - 0000-0003-1166-6206; @DrBarryChem

192 Barbora Balónová - 0000-0001-9029-5460; @BarboraBalonova

Supplementary Material

Supplementary material, including synthetic procedures, characterization data, ^{1}H NMR titration
studies, and UV-vis absorption spectroscopic data can be found online at:

Data Availability Statement

The datasets that underpin this work can be found in the University of New Brunswick Dataverse:
https://doi.org/10.25545/6TZWCG

References

200 Balónová, B.; Martir, D. R.; Clark, E. R.; Shepherd, H. J.; Zysman-Colman, E.; Blight, B. A. (2018)
201 Influencing the Optoelectronic Properties of a Heteroleptic Iridium Complex by Second-Sphere H-
202 Bonding Interactions. *Inorg. Chem.* 57, 8581–8587. doi: 10.1021/acs.inorgchem.8b01326

203 Balónová, B.; Shepherd, H. J.; Serpell, C. J.; Blight, B. A. (2020) IrIII as a Strategy for
204 Preorganisation in H-Bonded Motifs. *Supramol. Chem.* 32, 1–12. doi:
205 10.1080/10610278.2019.1649674

206 Blight, B. A.; Camara-Campos, A.; Djurdjevic, S.; Kaller, M.; Leigh, D. A.; McMillan, F. M.;
207 McNab, H.; Slawin, A. M. Z. (2009) AAA−DDD Triple Hydrogen Bond Complexes. *J. Am. Chem.*
208 *Soc.* 131, 14116–14122. doi: 10.1021/ja906061v

209 Blight, B. A.; Hunter, C. A.; Leigh, D. A.; McNab, H.; Thomson, P. I. T. (2011) An AAAA–DDDD
210 Quadruple Hydrogen-Bond Array. *Nat. Chem.* 3, 244–248. doi: 10.1038/nchem.987

211 Blondeau, P.; Segura, M.; Pérez-Fernández, R.; de Mendoza, J. (2007) Molecular Recognition of
212 Oxoanions Based on Guanidinium Receptors. *Chem. Soc. Rev.* 36, 198–210. doi: 10.1039/B603089K

213 Braga, D.; Maini, L.; Grepioni, F.; De Cian, A.; Félix, O.; Fischer, J.; Hosseini, M. W. (2000)
214 Charge-Assisted N–H(+)···O(−) and O–H···O(−) Hydrogen Bonds Control the Supramolecular
215 Aggregation of Ferrocenedicarboxylic Acid and Bis-Amidines. *New J. Chem.* 24, 547–553. doi:
216 10.1039/B002061N

217 Braga, D.; Polito, M.; Grepioni, F. (2004) Novel Organometallic Building Blocks for Molecular
218 Crystal Engineering. 3. Synthesis, Characterization, and Hydrogen Bonding of the Crystalline Mono-
219 and Bis-Amide Derivatives of [CoIII(H5-C5H4-COOH)2]+ and of the Cationic Zwitterion
220 [CoIII(H5-C5H4CONHC5H. *Cryst. Growth Des.* 4, 769–774. doi: 10.1021/cg049942w

221 Chowdhury, S. C.; Gillespie, J. W. (2018) A Molecular Dynamics Study of the Effects of Hydrogen
222 Bonds on Mechanical Properties of Kevlar® Crystal. *Comput. Mater. Sci.* 148, 286–300. doi:
223 10.1016/j.commatsci.2018.02.055

224 Djurdjevic, S.; Leigh, D. A.; McNab, H.; Parsons, S.; Teobaldi, G.; Zerbetto, F. (2007) Extremely
225 Strong and Readily Accessible AAA−DDD Triple Hydrogen Bond Complexes. *J. Am. Chem. Soc.*
226 129, 476–477. doi: 10.1021/ja067410t

227 Félix, O.; Hosseini, M. W.; De Cian, A.; Fischer, J. (2000) Crystal Engineering of 2-D Hydrogen
228 Bonded Molecular Networks Based on the Self-Assembly of Anionic and Cationic Modules. *Chem.*
229 *Commun.* 4, 281–282. doi: 10.1039/A909093B

230 Gale, P. A.; Pérez-Tomás, R.; Quesada, R. (2013) Anion Transporters and Biological Systems. *Acc.*
231 *Chem. Res.* 46, 2801–2813. doi: 10.1021/ar400019p

232 Han, J.; Yau, C.-W.; Lam, C.-K.; Mak, T. C. W. (2008) Designed Supramolecular Assembly of
233 Hydrogen-Bonded Anionic Rosette Layers. *J. Am. Chem. Soc.* 130, 10315–10326. doi:
234 10.1021/ja802425q

235 Horovitz, A.; Serrano, L.; Avron, B.; Bycroft, M.; Fersht, A. R. (1990) Strength and Co-Operativity
236 of Contributions of Surface Salt Bridges to Protein Stability. *J. Mol. Biol.* 216, 1031–1044. doi:
237 10.1016/S0022-2836(99)80018-7

238 Jorgensen, W. L.; Pranata, J. (1990) Importance of Secondary Interactions in Triply Hydrogen
239 Bonded Complexes: Guanine-Cytosine vs Uracil-2,6-Diaminopyridine. *J. Am. Chem. Soc.* 112,
240 2008–2010. doi: 10.1021/ja00161a061

241 Kuhn, B.; Mohr, P.; Stahl, M. (2010) Intramolecular Hydrogen Bonding in Medicinal Chemistry. *J.*
242 *Med. Chem.* 53, 2601–2611. doi: 10.1021/jm100087s

243 Lee, D. H.; Lee, H. Y.; Hong, J.-I. (2002) Anion Sensor Based on the Indoaniline–Thiourea System.
244 *Tetrahedron Lett.* 43, 7273–7276. doi: 10.1016/S0040-4039(02)01455-7

245 Leigh, D. A.; Robertson, C. C.; Slawin, A. M. Z.; Thomson, P. I. T. (2013) AAAA-DDDD
246 Quadruple Hydrogen-Bond Arrays Featuring NH···N and CH···N Hydrogen Bonds. *J. Am. Chem.*
247 *Soc.* 135, 9939–9943. doi: 10.1021/ja404504m

248 Linares Mendez, I. J.; Pleizier, J. S.; Wang, H.-B.; Wisner, J. A. (2019) ^{1}H NMR-Based Method for
249 the Determination of Complexation Equilibrium Parameters and Chemical Shifts in a Hydrogen-
250 Bonded System with Dynamic Composition. *J. Phys. Org. Chem.* 31, e3805. doi: 10.1002/poc.3805

251 Liu, L.; Zou, D.; Zhang, Y.; Zhang, D.; Zhang, Y.; Zhang, Q.; Wang, J.; Zeng, S.; Wang, C. (2019)
252 Assembly of Three Pharmaceutical Salts/Cocrystals of Tetrahydroberberine with Sulfophenyl Acids:
253 Improving the Properties by Formation of Charge-Assisted Hydrogen Bonds. *New J. Chem.* 43,
254 4886–4894. doi: 10.1039/C9NJ00131J

255 Marechal, Y. (2007) The Hydrogen Bond and the Water Molecule: Thephysics and chemistry of
256 water, aqueous and bio media; Elsevier Science & Technology: Amsterdam, Netherlands.

257 Moran, L. A.; Horton, H. R.; Scrimgeour, K. G.; Perry, M. D (2012) Principles of Biochemistry, 5th
258 ed.; Pearson Education: New York.

259 Nonoyama, M. (1974) Benzo[h]Quinolin-10-Yl-N Iridium(III) Complexes. *Bull. Chem. Soc. Jpn.* 47,
260 767–768. doi: 10.1246/bcsj.47.767

261 Persch, E.; Dumele, O.; Diederich, F. (2015) Molecular Recognition in Chemical and Biological
262 Systems. *Angew. Chem. Int. Ed.* 54, 3290–3327. doi: 10.1002/anie.201408487

263   Papmeyer, M.; Vuilleumier, C. A.; Pavan, G. M.; Zhurov, K. O.; Severin, K. (2016) Molecularly
264   Defined Nanostructures Based on a Novel AAA-DDD Triple Hydrogen-Bonding Motif. *Angew.*
265   *Chem.* 128, 1717-1721. doi: 10.1002/anie.201510423

266   Papoutsakis, D.; Kirby, J. P.; Jackson, J. E.; Nocera, D. G. (1999) From Molecules to the Crystalline
267   Solid: Secondary Hydrogen-Bonding Interactions of Salt Bridges and Their Role in Magnetic
268   Exchange. *Chem. Eur. J.* 5, 1474–1480. doi: 10.1002/(SICI)1521-3765(19990503)5:5<1474::AID-
269   CHEM1474>3.0.CO;2-T

270   Pop, L.; Hadade, N. D.; van der Lee, A.; Barboiu, M.; Grosu, I.; Legrand, Y.-M. (2016) Occurence of
271   Charge-Assisted Hydrogen Bonding in Bis-Amidine Complexes Generating Macrocycles. *Cryst.*
272   *Growth Des.* 16, 3271–3278. doi: 10.1021/acs.cgd.6b00246

273   Pranata, J.; Wierschke, S. G.; Jorgensen, W. L. (1991) OPLS Potential Functions for Nucleotide
274   Bases.Relative Association Constants of Hydrogen-Bonded Base Pairs in Chloroform. *J. Am. Chem.*
275   *Soc.* 113, 2810–2819. doi: 10.1021/ja00008a002

276   Prins, L. J.; Reinhoudt, D. N.; Timmerman, P. (2001) Non-covalent Synthesis Using Hydrogen
277   Bonding. *Angew. Chem. Int. Ed.* 40, 2382–2426. doi: 10.1002/1521-
278   3773(20010702)40:13<2382::AID-ANIE2382>3.0.CO;2-G

279   Sartorius, J.; Schneider, H.-J. (1996) A General Scheme Based on Empirical Increments for the
280   Prediction of Hydrogen-Bond Associations of Nucleobases and of Synthetic Host–Guest Complexes.
281   *Chem. Eur. J.* 2, 1446–1452. doi: 10.1002/chem.19960021118

282   Schmuck, C.; Wienand, W. (2003) Highly Stable Self-Assembly in Water: Ion Pair Driven
283   Dimerization of a Guanidiniocarbonyl Pyrrole Carboxylate Zwitterion. *J. Am. Chem. Soc.* 125, 452-
284   459. doi: 10.1021/ja028485+

285   Taylor, R.; Kennard, O. (1984) Hydrogen-Bond Geometry in Organic Crystals. *Acc. Chem. Res.* 17,
286   320–326. doi: 10.1021/ar00105a004

287   Thordarson, P. (2011) Determining Association Constants from Titration Experiments in
288   Supramolecular Chemistry. *Chem. Soc. Rev.* 40, 1305−1323.

289   Wang, H.; Gurau, G.; Shamshina, J.; Cojocaru, O. A.; Janikowski, J.; MacFarlane, D. R.; Davis, J.
290   H.; Rogers, R. D. (2014) Simultaneous Membrane Transport of Two Active Pharmaceutical
291   Ingredients by Charge Assisted Hydrogen Bond Complex Formation. *Chem. Sci.* 5, 3449–3456. doi:
292   10.1039/C4SC01036A

293